Available online at www.sciencedirect.com
SCIENCE DIRECT®
Journal of Crystal Growth 264 (2004) 31–35
JOURNAL OF CRYSTAL GROWTH
www.elsevier.com/locate/jcrysgro

Mn implanted GaAs by low energy ion beam deposition

Shu-Lin Song[a,*], Nuo-Fu Chen[a,b], Jian-Ping Zhou[a], Zhi-Gang Yin[a], Yan-Li Li[a], Shao-Yan Yang[a], Zhi-Kai Liu[a]

[a] *Key Laboratory of Semiconductor Materials Science, Institute of Semiconductors, Chinese Academy of Sciences, Beijing 100083, China*
[b] *National Micro gravity Laboratory, Institute of Mechanics, Chinese Academy of Sciences, Beijing 100080, China*

Received 13 October 2003; accepted 21 December 2003
Communicated by M. Schieber

Abstract

High dose Mn was implanted into semi-insulating GaAs substrate to fabricate embedded ferromagnetic Mn–Ga binary particles by mass-analyzed dual ion beam deposit system at room temperature. The properties of as-implanted and annealed samples were measured with X-ray diffraction, high-resolution X-ray diffraction to characterize the structural changes. New phase formed after high temperature annealing. Sample surface image was observed with atomic force microscopy. All the samples showed ferromagnetic behavior at room temperature. There were some differences between the hysteresis loops of as-implanted and annealed samples as well as the cluster size of the latter was much larger than that of the former through the surface morphology.

PACS: 51.60.+a; 72.80.Ga; 81.05.Zx; 81.15.Hi

Keywords: A1. X-ray diffraction; A3. Ion beam deposit; B2. Magnetic materials; B2. Semiconducting gallium arsenide

1. Introduction

The discovery of ferromagnetism in $Ga_{0.947}Mn_{0.053}As$ [1] with $T_c = 110$ K has triggered great interest on the study of III–V-based diluted magnetic semiconductors (DMS), which can make use of the spin degree of carriers. There are many studies concentrated on the origin of ferromagnetism [2–4] and characterizations of DMS [5–7]. Among those III–V-based DMS, GaMnAs was the most extensively studied because it provides the promise of combining magnetic phenomena with high-speed electronics and optoelectronics. However, the ferromagnetic transition temperature of GaMnAs is still far below room temperature because large amount of As could be incorporated to reduce the carrier mediated ferromagnetic interaction during the low temperature molecular beam epitaxy growth process [8]. On the other hand, ion implantation is also capable of introducing dopant concentrations above the usual equilibrium solid solubility limit. GaN based DMS has been successfully fabricated by implantation [9–11] while study on GaAs based DMS by implantation is still too limited after acquiring some results [12–14].

*Corresponding author. Tel.: +86-10-82304417; fax: +86-10-82304469.
E-mail address: slsong@red.semi.ac.cn (S.-L. Song).

0022-0248/$ - see front matter © 2004 Elsevier B.V. All rights reserved.
doi:10.1016/j.jcrysgro.2003.12.039

High dose Mn implantation could fabricate ferromagnetic Mn–Ga binary particles embedded in GaAs substrate. New ferromagnetic phase formed after annealing so it was a good point to study the relationship between saturation magnetization and annealing condition.

Sample structure was studied by using X-ray diffraction (XRD). The surface morphology was investigated with atomic force microscope (AFM). Structural symmetry of GaAs (0 0 4) was further determined from rocking curves by high-resolution X-ray diffraction (HRXRD). An alternating gradient magnetometer (AGM) was used to measure the samples magnetic properties.

2. Material preparation

The sample was prepared by low-energy dual ion beam deposit system with the mass selection function, which can purify the ions and even select isotopes to implant into the substrate. Mn ion beams were produced by Bernas type ion source. More detailed information was elaborated about this apparatus in Ref. [15]. Only one ion beam system was employed to implant Mn ions into the substrate with low energy in this experiment. The semi-insulating GaAs (1 0 0) were used as substrate which were cleaned in ethanol, acetone, and deionized water for 5 min each with ultrasonic vibration, then they were etched in H_2SO_4:H_2O_2:-H_2O (6:1:1) solvent. Finally, they were rinsed in deionized water and loaded into the growth chamber.

The growth process followed two steps at room temperature. Firstly, Mn ions were uniformly implanted into the substrate at high dose of $7.5 \times 10^{17}\,cm^{-2}$ with an acceleration voltage of 1000 V. Secondly, the growth energy lowered down to deposit Mn layer on GaAs surface to avoid the out-diffusion of Mn during annealing process.

The samples were cleaved into $10 \times 10\,mm^2$ and covered with Si substrate during the furnace annealing process at the range from 400°C to 800°C for 20 min each, 800°C for 60 min in N_2 forming gas while the temperature was monitored and controlled by a thermocouple located close to the Si substrate inside the annealing chamber. In this paper, we mainly focus on the comparison between as-implanted and 60 min-annealed samples.

3. Results and discussion

3.1. Structural analyses

XRD measurements of the Mn implanted GaAs samples were performed on a Rigaku D/max-2400 diffractometer. The rotating Cu target was used with a voltage of 50 kV and a current of 150 mA, and the X-ray wavelength ($K\alpha = 1.54056$ Å)was selected by using a (0002) graphite crystal scattering at the receiving goniometer slit. The θ–2θ pattern scans with a step size of $2\theta = 0.02°$ at room temperature.

In addition to GaAs substrate main peaks (0 0 2) and (0 0 4), there were new phase peaks appeared from the XRD results Fig. 1. The hump next to GaAs (0 0 2) peak converted to MnO (1 0 0) peak after annealing. It is mainly for the annealing process can promote the recrystallization of the oxides, which formed after the deposited Mn layer exposed in air. The intensity of GaAs (0 0 2) peak greatly reduced from the XRD results comparison between the samples. The change of (0 0 4) peak will be further investigated with the help of rocking curve.

Three new Ga_5Mn_8 peaks appeared with (4 4 1) peak disappeared after the high temperature annealing process. It was clearly shown that annealing could also promote the formation of Mn–Ga binary phase, which was also confirmed from XRD results of samples with rapid thermal annealing (RTA) at 900°C for 5 min or the work by Chen et al. [13].

The X-ray rocking curves of GaAs (0 0 4) peaks for as-implanted and annealed samples were shown in Fig. 2. The measurements were carried out on a Philips X'pert-MRD (materials research diffractometer) with a Cu Kα radiation source and a triple-axis output monochromator by ω–2θ scanning. The system is also equipped with a fully rotational rocking curve stage so it allows measurement of off-axis reflections. Lattice mismatch

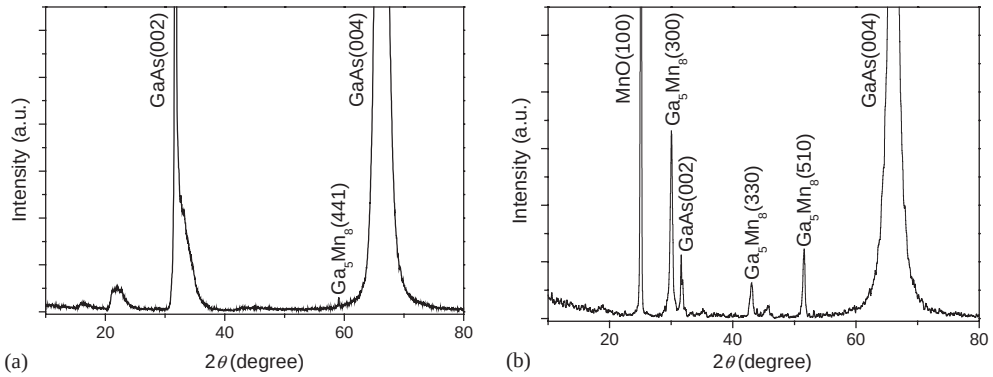

Fig. 1. X-ray diffraction pattern: (a) as-implanted sample and (b) annealed sample.

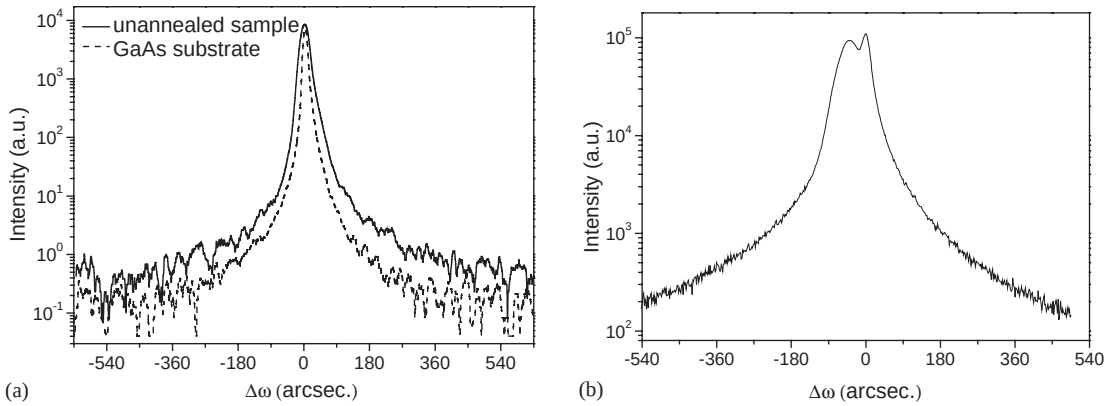

Fig. 2. Experimental GaAs (0 0 4) X-ray rocking curves: (a) comparison between as-implanted sample and GaAs substrate and (b) annealed sample.

measurements were made by X-ray rocking curves, which are very sensitive in detecting the damage by ion implantation. Rocking curve of the Mn implanted sample was more asymmetric than that of unimplanted GaAs substrate.

As for the annealed sample, the full-width at half-maximum (FWHM) of (0 0 4) peak greatly differed from that of the as-implanted sample. There were two peaks from the rocking cure though they were not separated completely. It was mainly for the strain of the implanted layer relaxed after the high temperature annealing process. The rocking curves of high temperature annealed sample were also different with that of low temperature annealed sample from their symmetries.

3.2. Surface morphology

Atomic force microscopy is a method of measuring surface topography on a scale from angstroms to 100 μm. The technique enables to image a sample surface to deliver three-dimensional realistic impressions. There were many island-like humps on as-implanted sample surface from Fig. 3 with a RMS of 3.529 nm on $5 \times 5\,\mu m^2$ surface scanning area. The surface of the annealed sample surface was much rough with a RMS of 13.182 nm. The surface roughness was in close relationship with the formation of new phase. This was corroborated with scanning electron microscopy (SEM) and energy dispersive spectrometer (EDS) results, which will be published elsewhere.

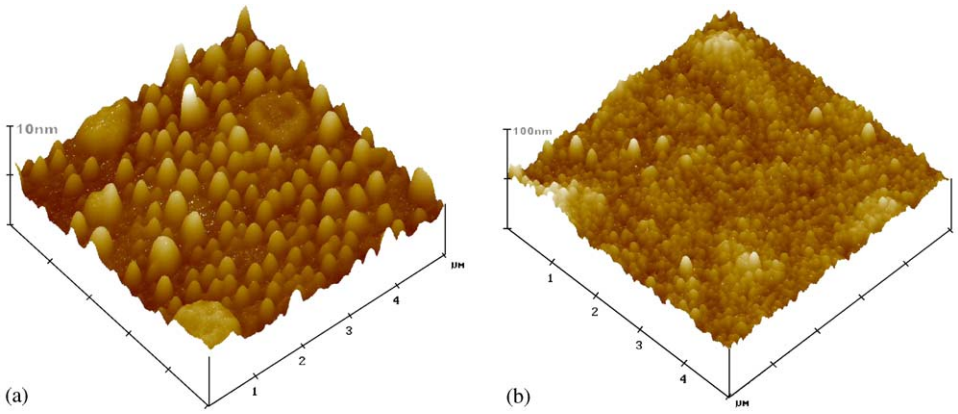

Fig. 3. AFM morphology of (a) as-implanted sample and (b) annealed sample.

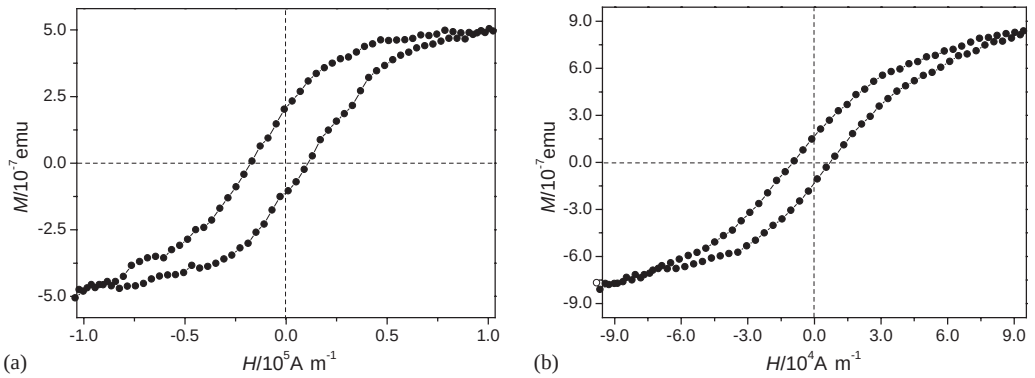

Fig. 4. Magnetic experimental data of (a) as-implanted sample and (b) annealed sample.

3.3. Magnetic property

Magnetic properties were measured by using a Model 2900 MicroMag™ AGM at room temperature. Both the as-implanted and annealed samples showed room-temperature ferromagnetic behavior from the AGM results. It was clearly shown that the saturation magnetization M_s increased after annealing though the M_s level was small from Fig. 4. The increase of M_s was in accordance with the formation of Ga_5Mn_8 or other undetected ferromagnetic Mn–Ga binary compounds because MnO was antiferromagnetic. The difference on hysteresis loops between the as-implanted and annealed samples may be the change in easy axis orientation after the high temperature annealing process.

Controlling the annealing time and temperature could change M_s may provide a new way to explore new tunable spin-dependent magneto-electronic and magneto-optical devices [12].

4. Conclusion

In summary, magnetic and structural properties of high dose Mn implanted GaAs were analyzed by different methods. It was shown that annealing process could recrystallize the Mn related oxides and promote the formation of Mn–Ga binary compounds. The increase of saturation magnetization results from the increase of Ga_5Mn_8 or the formation of other undetected compounds after annealing. This work could provide a new

prospect to study novel magnetic device based on annealing high dose Mn implanted GaAs.

Acknowledgements

This work was partially supported by National Natural Science Foundation of China 60176001, Special Funds for Major State Basic Research Projects G20000365 and G2002CB311905.

References

[1] H. Ohno, A. Shen, F. Matsukara, A. Iewa, A. Endo, Y. Iye, Appl. Phys. Lett. 69 (1996) 363.
[2] V.I. Litinov, V.K. Dugaev, Phys. Rev. Lett. 86 (2001) 5593.
[3] J. Schliemann, J. König, Hsiu-Hau, L. Allan, H. MacDonald, Appl. Phys. Lett. 78 (2001) 1550.
[4] T. Dietl, H. Ohno, F. Matsukura, J. Cibert, D. Ferrand, Science 287 (2000) 1019.
[5] X. Liu, Y. Sasaki, J.K. Furdyna, Appl. Phys. Lett. 79 (2001) 2414.
[6] T. Shono, T. Hasegawa, T. Fukumura, F. Matsukura, H. Ohno, Appl. Phys. Lett. 77 (2000) 1363.
[7] S. Zhang, Phys. Rev. Lett. 85 (2000) 393.
[8] S. Sanvito, N.A. Hilll, Appl. Phys. Lett. 78 (2001) 3493.
[9] S.J. Pearton, M.E. Overberg, G. Thaler, C.R. Abernathy, J. Vac. Sci. Technol. A. 20 (2002) 721.
[10] T. Sasaki, S. Sonoda, Y. Yamamoto, et al., J. Appl. Phys. 91 (2002) 7911.
[11] A.Y. Polyakov, N.B. Smirnov, A.V. Govorlov, et al., J. Appl. Phys. 93 (2003) 6388.
[12] Jing Shi, J.M. Kikkawa, R. Proksch, et al., Nature 377 (1995) 707.
[13] Chenjia Chen, Ming Cai, Xuezhong Wang, et al., J. Appl. Phys. 87 (2000) 5636.
[14] M.A. Scarpulla, O.D. Dubon, K.M. Yu, et al., Appl. Phys. Lett. 82 (2003) 1251.
[15] F.-g. Qin, X.-m. Wang, Z.-k. Liu, et al., Rev. Sci. Instrum. 62 (1991) 2322.